Advanced Materials Research *Online: 2013-03-11*
ISSN: 1662-8985, Vol. 667, pp 10-23
doi:10.4028/www.scientific.net/AMR.667.10

New EM Transmitter with $Y_3Fe_5O_{12}$ based Magnetic Feeders Potentially Used for Seabed Logging Application

Majid Niaz Akhtar [1,2,a], Noorhana Yahya[3,b], and Nadeem Nasir[1,c]

[1]Department of Electrical and Electronic Engineering, Universiti Teknologi PETRONAS, Bandar Seri Iskandar, 31750 Tronoh, Perak, Malaysia.

[2]Department of Physics, Comsats Institute of Information Technology, Lahore, Pakistan.

[3]Department of Fundamental and Applied Sciences Engineering, Universiti Teknologi PETRONAS, Bandar Seri Iskandar, 31750 Tronoh, Perak, Malaysia.

[a]majidniazakhtar@gmail.com, [b]noorhana_yahya@petronas.com.my, [c]nadeemntu@hotmail.com

Keywords: Self combustion, Nanoparticles, X-ray diffraction, Field emission scanning electron microscopy, Q-factor and EM transmitter.

Abstract. Sea bed logging (SBL) is a new technique for detection of deep target hydrocarbon reservoir. Powerful electromagnetic (EM) transmitter is required for the transmission of EM signal underneath the seabed. New aluminum transmitter with yttrium iron garnet ($Y_3Fe_5O_{12}$) based magnetic feeders was used in a scale tank to increase the magnitude of the magnetic field. Yttrium iron garnet samples were prepared using self combustion technique at different sintering temperatures of 750°C, 950°C and 1150°C. Characterizations of $Y_3Fe_5O_{12}$ samples were done by using XRD, RAMAN, FESEM and Impedence network analyser. X-ray diffraction results revealed that yttrium iron garnet phase with good crystallinity appeared at sintering temperature of 1150°C. Nanoparticles size ranging from 60 to 110 nm was investigated. Raman results also confirmed garnet structure of yttrium iron garnet at sintering temperature of 1150°C. Field emission scanning electron microscopy (FESEM) was used to image the morphology of the $Y_3Fe_5O_{12}$ nanoparticles. Magnetic properties of $Y_3Fe_5O_{12}$ magnetic feeders illustrates that $Y_3Fe_5O_{12}$ has high Initial permeability (58.054), high Q-factor (59.842) and low loss factor (0.0003) at sintering temperature of 1150°C. $Y_3Fe_5O_{12}$ magnetic feeders with high Q factor were chosen for new aluminum EM transmitter. Experiments with a scale factor of 2000 were carried out in scaled tank. It was found that Al transmitter with $Y_3Fe_5O_{12}$ magnetic feeders increased magnitude of magnetic field strength up to 180%.

Introduction

Hydrocarbon exploration is very expensive, not perfect and can be harmful to marine life due to large value of current used. A new technique of detecting hydrocarbon reservoirs has been developed and is called “seabed logging”. Seabed logging is an application that uses controlled source electromagnetic (CSEM) technique to detect and characterize hydrocarbon reservoirs in deep water areas [1-3].

The transmitter is supplied with appropriate current and frequency for the transmission of EM (electromagnetic) waves in the marine environment. Energy of the electromagnetic waves depends on the voltage and current supplied to the transmitter. Arrays of receivers are placed on the sea floor to measure both the amplitude and phase of the received signal. Different positions of the

transmitter and receivers are used to determine model of seafloor resistivity. Hydrocarbon reservoir has resistivity perhaps 10-100 times greater than seawater and other sediments. Transmitter that transmits the wave is controlled by the source power generator. Electromagnetic waves generated by the transmitter will be reflected and guided by the hydrocarbon reservoir because of its high resistance [4]. The magnetic feeders are used to excite the TM wave field components such as Hϕ , Ez, and Eρ. When the magnetic feeders are used on the wire antenna (conductor), the magnetic flux energy will be transfered from magnetic feeders to the current flowing along the antenna conductor. The higher the Q value gives higher efficiency of the power which is delivered to the antenna current. It was also reported that hysteresis losses and eddy current losses increases as the frequency increases [5].

Yttrium iron garnet ($Y_3Fe_5O_{12}$) is a well known attractive magnetic garnet used for microwave region as well as for circulators, optical isolators and many magnetic optical devices. Yttrium iron garnet has large Faraday rotation and high saturation magnetization and due to these properties, it has potential applications in electronic devices and in magnetic bubble domain-type digital memories [6]. Magnetic properties such as initial permeability, relative loss factor, saturation magnetization and remanence etc depend on the crystal structure and morphology of the garnet materials [7].

Many authors have focused their study on the physical and chemical properties and on the reduction of the particles size of the ferromagnetic garnet materials [8-9]. Non conventional (chemical) methods have been found out by many researchers for the preparations of soft ferrite with garnet structure. These methods have advantages over conventional methods were reported by [10-12]. Chemical methods were investigated much better due to their large surface area of nanoparticles relative to low sintering temperature with good homogeneity and high chemical purity etc. Self combustion synthesis [13], sol–gel route [14], hydrothermal precipitation [15], glass crystallization method [16], mechanical alloying [17], and chemical co-precipitation [18], etc are non conventional methods used to synthesize the nanoparticles of the yttrium iron garnet. In recent years, attentions have been made to develop a technique for the synthesis of well known iron garnet nanoparticles at low sintering temperature [19]. Self combustion method has certain advantages such as mixing of atomic scale with fast reaction rate at low sintering temperature.

Magnitude of electromagnetic (EM) waves for detection of hydrocarbon reservoir in marine environment is very important in seabed logging. New carbon nanotubes (CNT) fibres/aluminium based EM transmitter was developed and NiZn ferrite as magnetic feeders was used to evaluate the presence of oil. Single phase of $Ni_{0.76}Mg_{0.04}Zn_{0.2}Fe_2O_4$ was sintered at 700°C in air having [311] major peak was obtained by sol gel method. FESEM results showed average diameters of nanoparticles in ranges of 17-45 nm. High Q-factor (approximately 50) sample was used as magnetic feeders for the EM transmitter. It was observed that the magnitude of EM waves of this new EM transmitter increased up to 400% [20].

Seabed logging (SBL) has shown very promising results for the direct detection of hydrocarbon by an active source using electromagnetic (EM) energy. However, powerful horizontal electrical dipole (HED) which can generate powerful electromagnetic signal still remains a challenge. Development of twin dipole antenna with yttrium iron garnet based magnetic feeder is reported in this research work. The toroid shape yttrium iron garnet samples were prepared using sol gel method. XRD results revealed best garnet cubic phase giving (4 2 0) plane of the $Y_3Fe_5O_{12}$

crystallite appeared at 33.30. It was observed that by using the transmitter with the $Y_3Fe_5O_{12}$ magnetic feeder (UTP28), an improvement of peak to peak voltage of the EM detectors by more than 400 % was found. It could be seen that twin dipoles were able to detect EM waves at more than 70 meters. It was also observed that the dipole antenna has an ability to change from HED to vertical magnetic dipoles (VMD) mode [21].

The present work focuses on enthusiastic and efficient investigations on the garnets having chemical formula of $Y_3Fe_5O_{12}$ with greater homogeneity by using self combustion method. X-ray diffraction analysis, raman spectra, field emission scanning electron microscopy (FESEM) and magnetic characteristics of $Y_3Fe_5O_{12}$ nanoparticles were examined. Magnetic feeders were also fabricated using $Y_3Fe_5O_{12}$ nanoparticles. Al wire with $Y_3Fe_5O_{12}$ based magnetic feeders were used as EM transmitter for the improvement of magnitude verses offset in a scaled tank.

Methodology

Experimental Set up. The raw materials iron nitrate [$Fe(NO_3)_3.9H_2O$], and yttrium nitrate [$Y(NO_3)_3.6H_2O$] having 99.99% purity were used. All metal nitrates used for the synthesis of Yttrium iron garnet (YIG) were dissolved in the aqueous solution of 160 ml of citric acid [$C_6H_8O_7.H_2O$]. The solution was stirred at 250 r.p.m for 10 days and was combusted on the hot plate stirrer with gradual heating for 40 minutes until temperature was 110°C. The combusted material was dried in the oven at 100°C for 2 days and dried powder was grounded for 6 hours. The powder was sintered at 750°C, 950°C and 1150°C respectively for 4 hours. The yttrium iron garnet nanoparticles sintered at 950 °C and 1150 °C were moulded to a toroidal shape using hydraulic press at pressure of 50kN. 1% of zinc stearate acted as lubricant and 1% of PVA acted as binder were added into nanoparticles of yttrium iron garnet. $Y_3Fe_5O_{12}$ toroidal samples were then sintered at 1050°C and 1250 °C for 5 hours and 10 hours in air respectively. The phase and structure of the $Y_3Fe_5O_{12}$ nanoparticles were examined by X-ray diffractometer (Bruker D8 advance). Raman spectra were obtained for $Y_3Fe_5O_{12}$ at different temperatures by using Raman spectroscopy system with 514.5nm.The morphology and shape of the particles were characterized by using FESEM (SUPRA 35VP). Magnetic characteristics were carried out by using impedence vector network Analyzer (Agilent 4294 A) in the frequency range of 40 Hz – 110 MHz.

Scale tank with a scale factor of 2000 was constructed to investigate magnitude of B field from Al EM transmitter with and with out $Y_3Fe_5O_{12}$ based magnetic feeders in tab water. Aluminium wire was used as EM transmitter with $Y_3Fe_5O_{12}$ based ferrite as the magnetic feeders in the scale tank. Function generators were used to apply square wave with 20V peak to peak voltage to the EM transmitter. Magnetic field generated by EM transmitter was detected by fluxgate magnetic field sensors, Model Mag-03MSS100 (Bartington Instruments). Three magnetic sensors were placed at equal distance from each other. The magnitude of EM waves was recorded by a Decaport data acquisition system Model NI PXI-1042. Schematic diagram of lab scale with new EM transmitter with three sensors is shown in Fig.1.

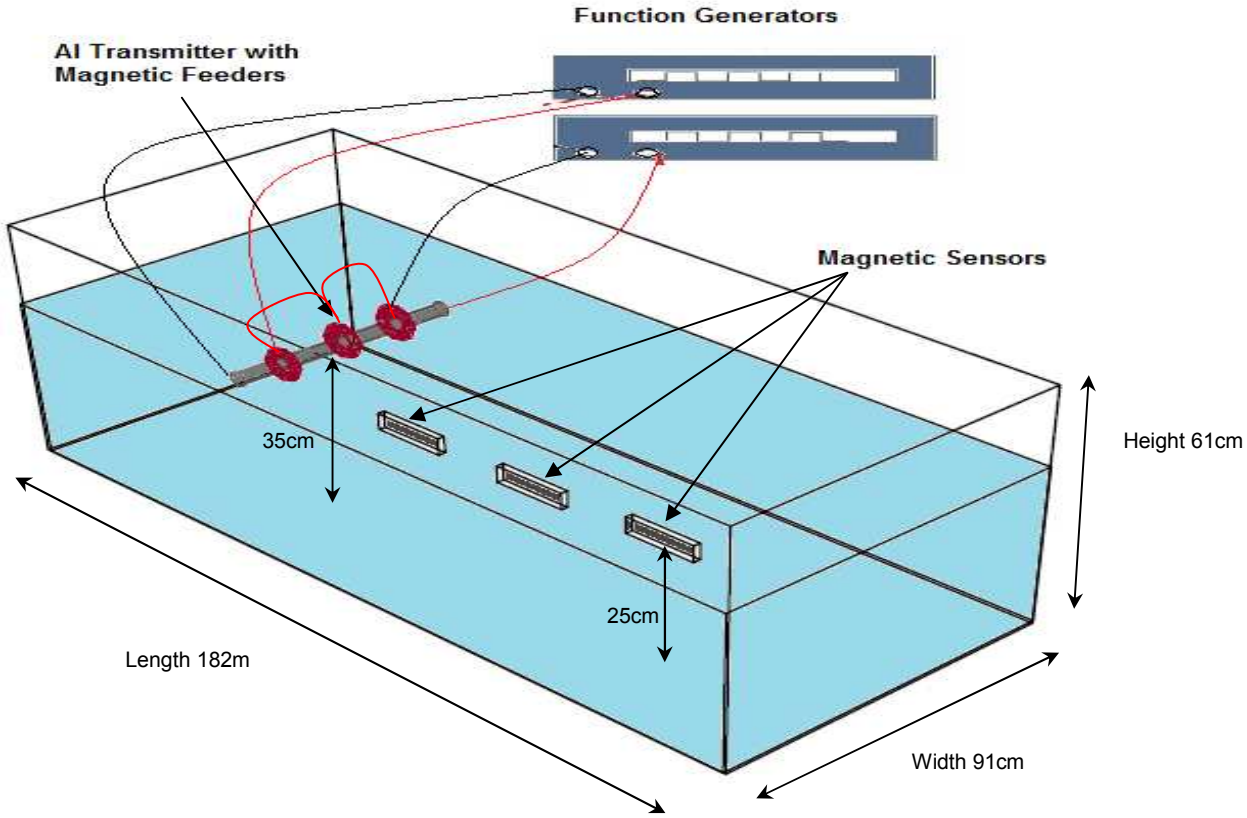

Fig. 1, Schematic Diagram of a Scaled Tank with New Al transmitter with $Y_3Fe_5O_{12}$ based magnetic feeders.

Scale factor Equations. Scale tank was constructed to validate the increase in magnitude of B field from new EM transmitter. Lab scale dimension (d_{lab}) and full scale dimensions (d_{fs}) are related to scale factor. In this case, water level of 1000m and overburden with also 1000m height replicates the marine environment in the scaled tank. Scale factor in this scale experiments was 2000 [22].

$$\frac{d_{fs}}{d_{lab}} = n \tag{1}$$

$$\left(\frac{\rho}{fd}\right)_{fs} = n^2 \left(\frac{\rho}{fd}\right)_{lab} \tag{2}$$

$$n^2 f_{fs} = f_{lab} \tag{3}$$

where f is the frequency of the transmitter, ρ is the conductivity of the medium, and d is height of the resistive layer. It can be seen that full scale dimension is equal to n times of the laboratory scale dimension.

Results and Discussions

X-Ray Diffraction (XRD). X-ray diffraction with CuKα with wavelength of λ=1.54056 ^{o}A was used to find out the crystal structure of yttrium iron garnet samples. Diffraction patterns of samples before sintering and sintering at 750 ^{o}C, 950 ^{o}C and 1150 ^{o}C are shown in Fig. 2.

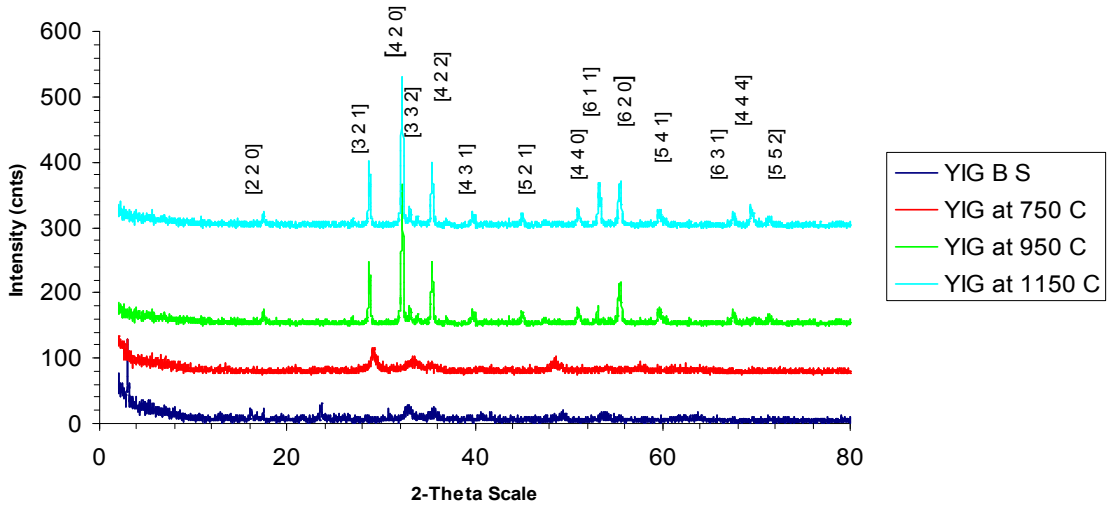

Fig.2, X-ray diffraction patterns of $Y_3Fe_5O_{12}$ (YIG) samples prepared by self combustion method.

$$D = \frac{K\lambda}{\omega \cos\theta} \tag{4}$$

where,
K= varies with hkl & crystallite shape equal to 0.9.
θ = Bragg's angle
ω =Full width at half maximum (FWHM)
λ = wavelength of incident radiation

From the diffraction patterns it has been shown that with out firing the yttrium iron garnet showed no peaks but as we increased temperature from 750°C to 1150°C the peaks increased. A clear diffraction line with sharp peak (420) designates high crystallinity of the $Y_3Fe_5O_{12}$ sintered sample at 1150°C showed single phase $Y_3Fe_5O_{12}$ garnet structure. All peaks were exactly matched with the standard JCPDS card 77-1888. Many authors have reported this peak for single phase yttrium iron garnet structure [23]. The average crystallite size of the $Y_3Fe_5O_{12}$ sintered samples were calculated from broadening of [420] peak using the sherrer formula as given in (Equation 1). The crystallite sizes showed variation from 60 nm to 100nm for $Y_3Fe_5O_{12}$ sintered samples as temperature increased from 750°C, 950°C, and 1150°C respectively.

Raman Spectra. Raman spectra result of $Y_3Fe_5O_{12}$ sintering at temperatures 750°C, 950°C and 1150°C are shown in Fig. 3. Raman results also confirmed that as the sintering temperature increased raman peaks increased. Maximum raman shift occurs at 263 cm^{-1} which showed the growth of the grains after sintering at 1150 °C. The major bands for Raman shift of $Y_3Fe_5O_{12}$ are 188, 273, 329, and 510 cm^{-1}[24].

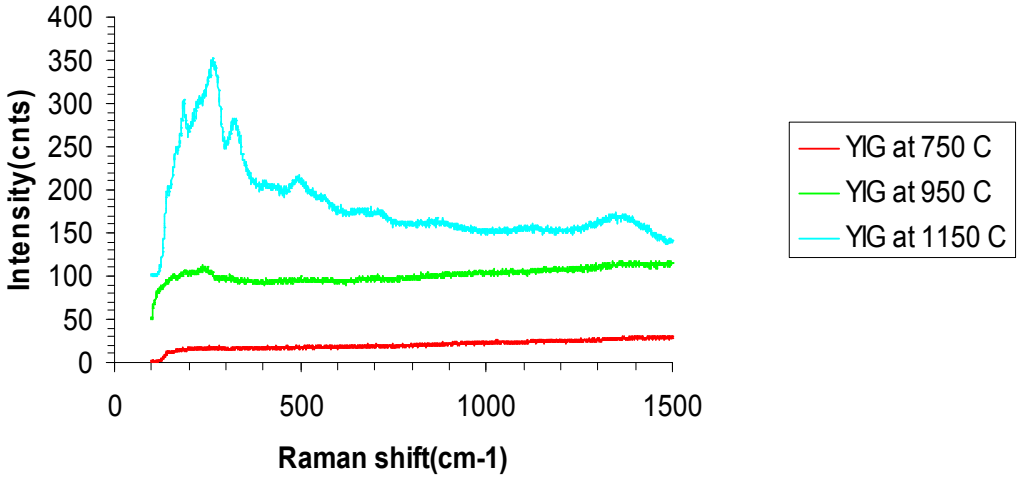

Fig. 3, Raman spectra results of $Y_3Fe_5O_{12}$ (YIG) samples prepared by self combustion method.

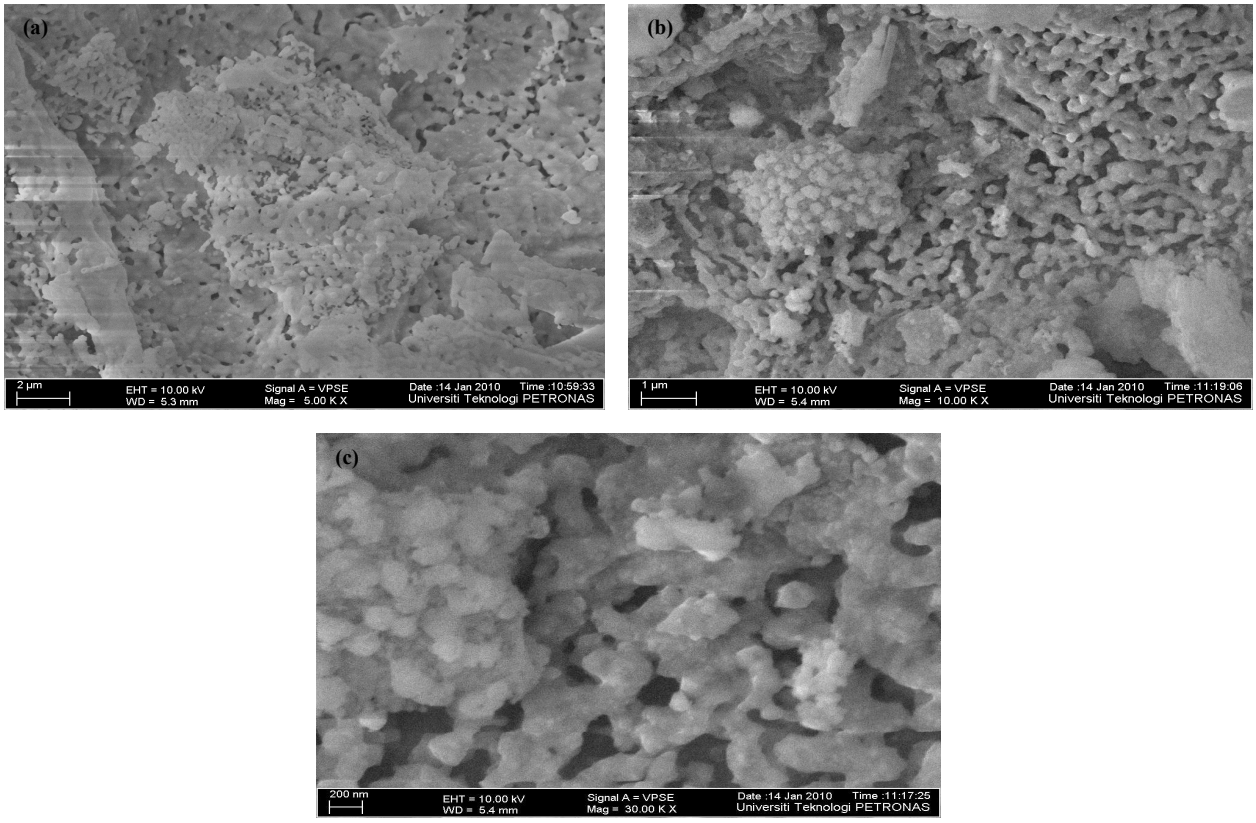

Fig. 4, FESEM micrographs of $Y_3Fe_5O_{12}$ ferrite powder at 750 °C (a) 5 KX (b) 10 KX (c) 30 KX.

FESEM results. Field Emission Scanning Electron Microscope (FESEM) was used to measure the dimensions of the grain size and morphology of the bulk and nanoparticles. FESEM graphs for $Y_3Fe_5O_{12}$ samples sintered at 750°C, 950°C and 1150°C at different resolutions are shown in Figs. (4-6). It has been observed from the results of FESEM that most of particles were agglomerated with other particles in a uniform manner. This may be due to large surface area and high surface energy of the $Y_3Fe_5O_{12}$ nanoparticles [25]. The pores in $Y_3Fe_5O_{12}$ sintered samples at 750°C and 950°C prevented atoms from diffusing which results noncrystalline powder as confirmed by XRD results. Porous features after sintering of the $Y_3Fe_5O_{12}$ samples indicated easy breaking of agglomeration at higher temperature [26].There was no agglomerations in $Y_3Fe_5O_{12}$ sample sintered

at 1150°C which shows uniform grain structure (Fig. 6). It was attributed that change in the particle size and morphology of $Y_3Fe_5O_{12}$ samples sintered at 750°C, 950°C, and 1150°C was due to the breaking and welding of particles. It was reported that Yttrium iron ions have large ionic radii (0.892°A) than the ferrum ions (0.65°A). So ferrum ions went to tetrahedral and octahedral sites where as yttrium ions goes to dodecahedral sites (2.40°A) [27]. The grain size of the sample also increased as we increased temperature from 750°C to 1150°C. It was also investigated that the grain size of $Y_3Fe_5O_{12}$ prepared by self combustion method was less in sizes as compared to the samples prepared by conventional method [28].

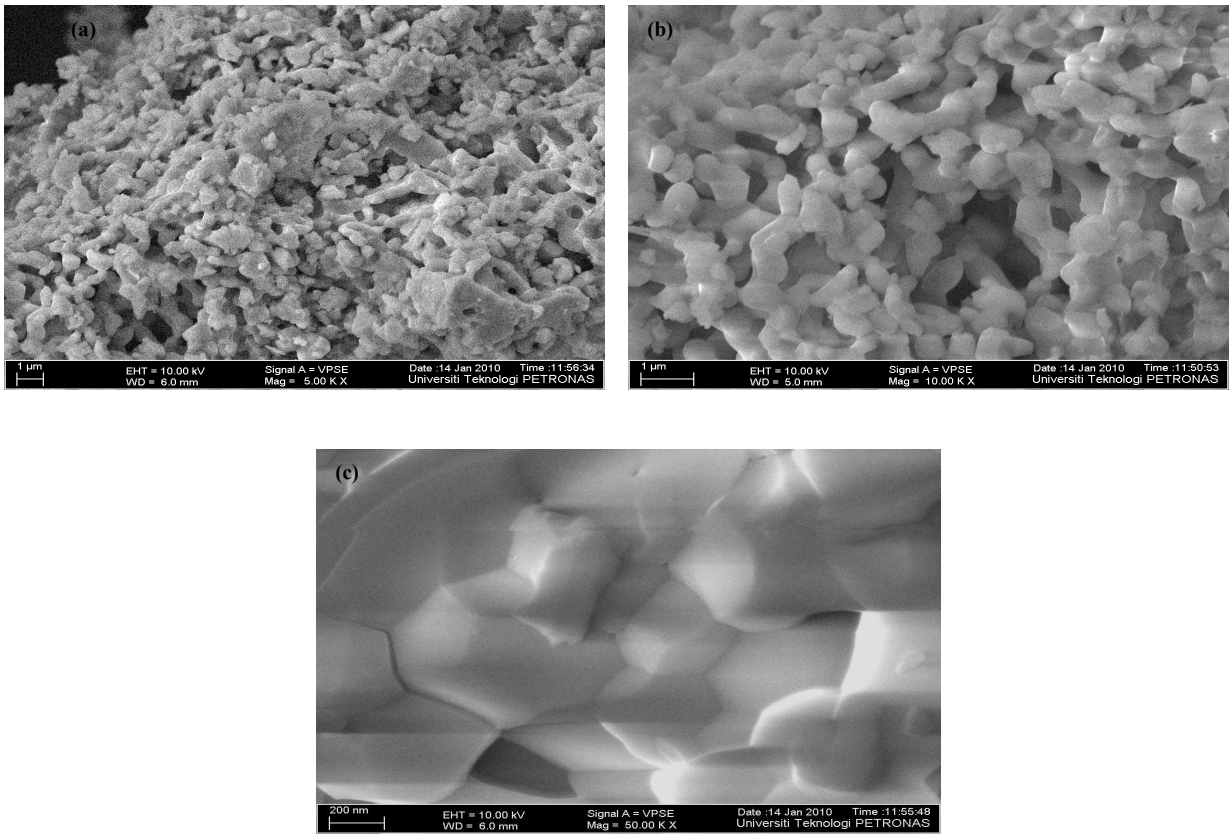

Fig. 5, FESEM micrographs of $Y_3Fe_5O_{12}$ ferrite powder at 950 °C (a) 5 KX (b) 10 KX (c) 50 KX.

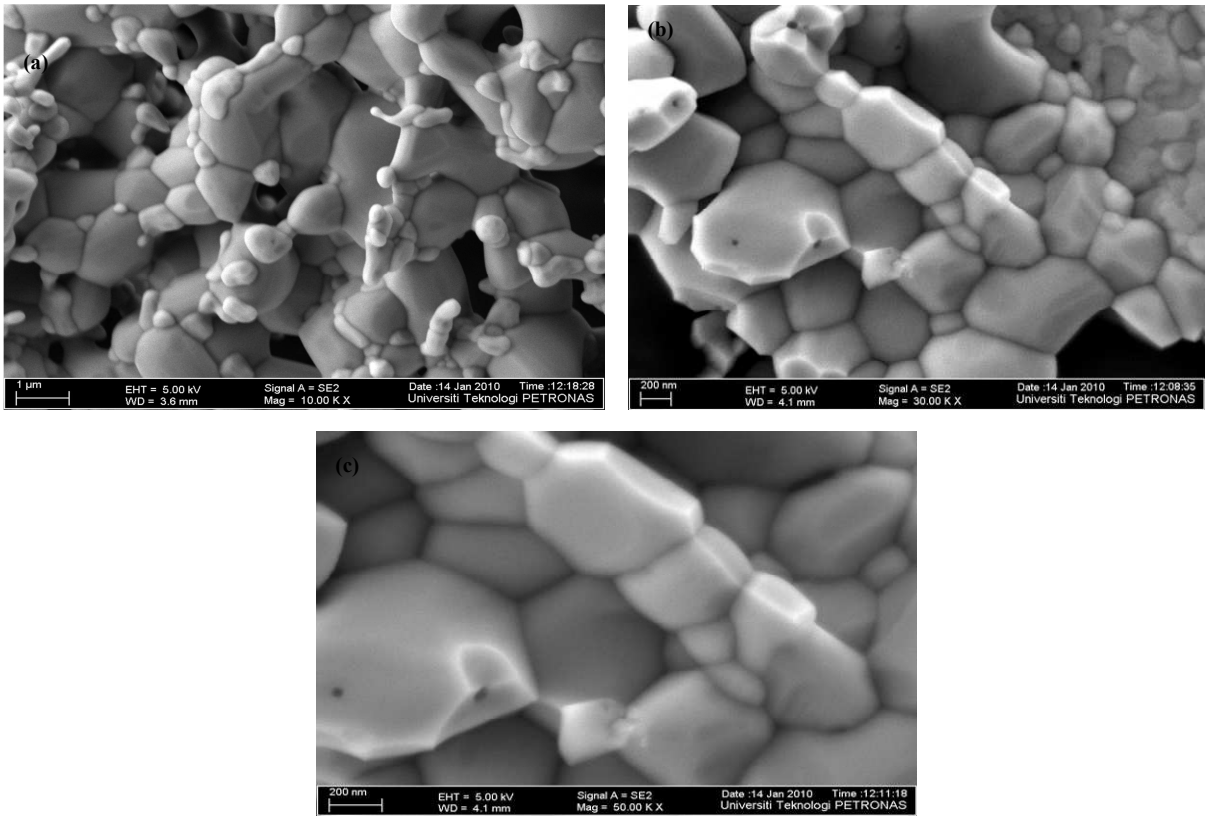

Fig. 6, FESEM micrographs of $Y_3Fe_5O_{12}$ ferrite powder at 1150 °C (a) 10KX (b) 30 KX (c) 50 KX.

EDX Analysis. The EDX results of $Y_3Fe_5O_{12}$ samples showed that the iron oxygen, and yttrium elements were with atomic percentages of 22.41%, 67.18% and 10.41%, respectively as given in Table 1. From Fig. 7 and Table 1 we can see that there is no impurity observed due to high purity of the starting materials for the preparation of the $Y_3Fe_5O_{12}$ nanoparticles. The higher peak of the oxygen in the spectrum indicated high concentration as compared to the ferum element of the $Y_3Fe_5O_{12}$.

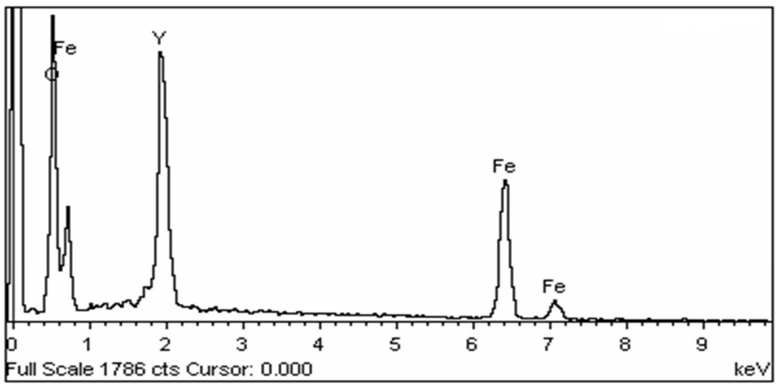

Fig. 7, EDX spectrum of $Y_3Fe_5O_{12}$ ferrite powder.

Table. 1, EDX of $Y_3Fe_5O_{12}$ ferrite powder.

Element	Weight%	Atomic%
O K	33.05	67.18
Fe K	38.48	22.41
Y L	28.47	10.41
Total	100.00	

Initial permeability, Q factor and Loss factor. Series values of inductance, L_s and Q factor were recorded from the lowest frequency to resonance frequencies from the impedence vector network Analyzer (Agilent 4294 A). Initial permeability, Q-factor and relative loss factor (RLF) of $Y_3Fe_5O_{12}$ sintered at 750°C 950°C and 1150°C were calculated using network analyser. The formula for Initial permeability μ_i is

$$\mu_i = \frac{2\pi L_S}{N^2 \mu_o t \ln(Do / Di)} \quad (5)$$

Where Ls is the parallel inductance, N is the number of turns, t is the thickness of toroid, μ_0 is the permeability of free space ($4\pi \times 10^{-7}$ m/A), D_0 is the outer diameter, and D_i is the inner diameter of the toroid, respectively. The initial permeability increases with increasing of frequency where relative loss factor (RLF) decreases as the frequency is increasing are shown in Figs. 8(a,c). Comparison of initial permeability, Q factor and loss factor at temperature of 750°C, 950°C and 1150°C are given in Table 2. It has been investigated by many researchers that ferrite materials have higher Initial permeability due to bulk density and large grain size [29]. Bulk density increases due to pores and also raises its spin rotational contribution which also contributes to increase permeability [30]. Q factor of $Y_3Fe_5O_{12}$ sample sintered at 1150°C showed highest value (59.842) at resonance frequency of 14 MHz than $Y_3Fe_5O_{12}$ sample sintered at 950°C (50.570) and 750°C (36.489) as shown in Fig. 8(b). The initial permeability increased due to less interruption between domain walls, which may be due to decrease in magnetic anisotropy, internal stress and crystal anisotropy at higher temperature. The surface morphology, density, porosity, grain size, Fe^{+2} content and single phase structure of the ferrite may affect the initial permeability. Relative loss factor is the ratio of tanδ to initial permeability. Relative loss factor is measured from 1 kHz to 1 MHz as suggested by many authors [30-31]. The relative loss factor is seen to be decreasing up to 10 MHz and after this it remains smooth. The frequency at which relative loss factor decreases and has minimum value is called threshold frequency. The low loss factor value indicates high purity of samples obtained by non conventional (wet) method [31].

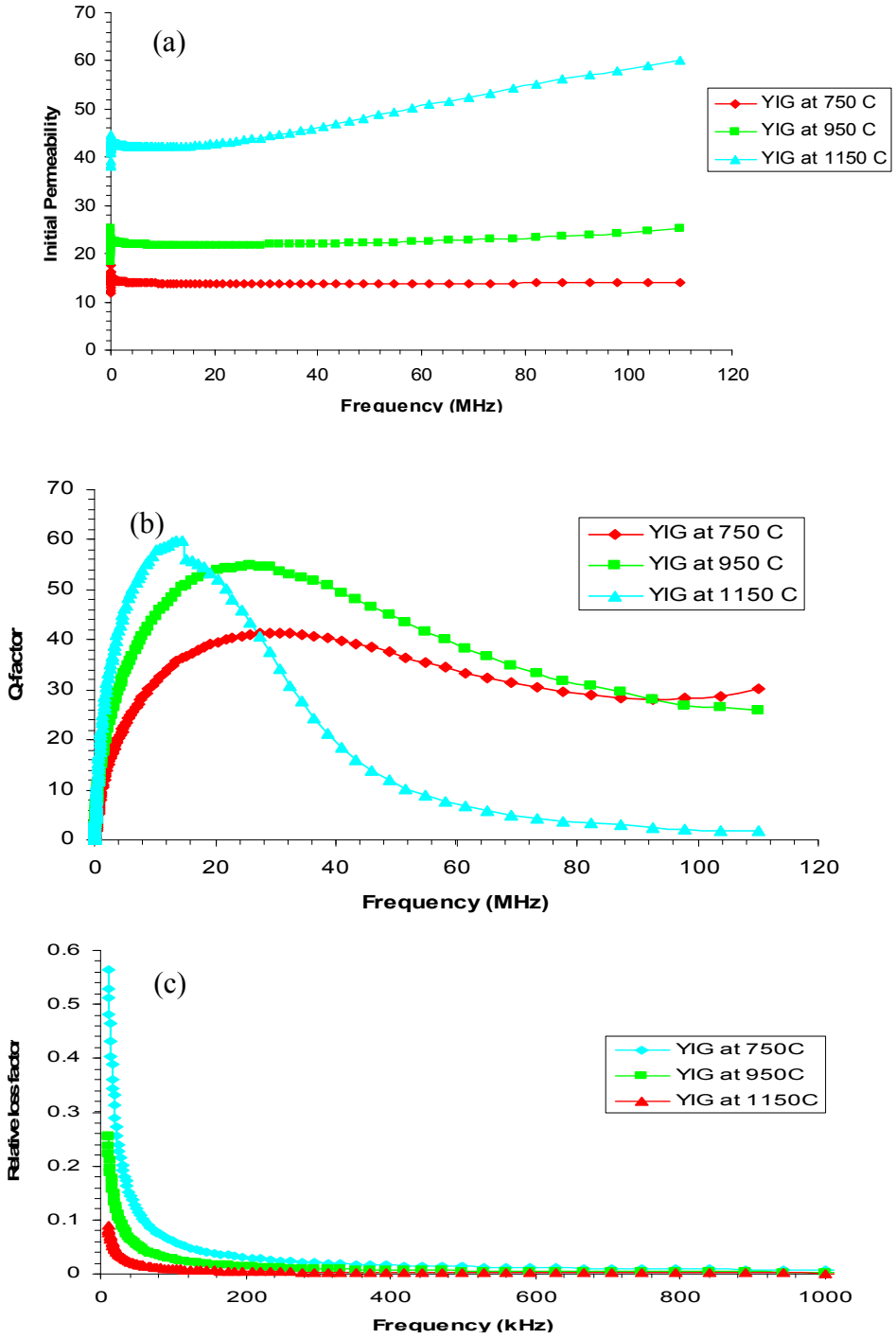

Fig. 8, (a) Initial Permeability,(b) Q factor and (c) relative loss factor of $Y_3Fe_5O_{12}$ (YIG) magnetic feeders at 750°C, 950°C and 1150°C.

Table 2: Initial permeability, Q factor and relative loss factor of $Y_3Fe_5O_{12}$ at 750 °C, 950 °C and 1150 °C.

Samples	Initial permeability at	Q-factor at	Relative loss factor at	
	100 MHz	14 MHz	100 kHz	13 MHz
$Y_3Fe_5O_{12}$ at 750 °C	13.981	36.489	0.030	0.0020
$Y_3Fe_5O_{12}$ at 950 °C	24.250	50.570	0.026	0.0009
$Y_3Fe_5O_{12}$ at 1150 °C	58.054	59.842	0.008	0.0003

EM transmitter comparison was done by Al wire transmitter without and with $Y_3Fe_5O_{12}$ based ferrite as magnetic feeders synthesized at 1150 °C in a designed scale tank. Magnitude verses offset of Al transmitter and Al transmitter with $Y_3Fe_5O_{12}$ magnetic feeders was measured to investigate the effect of $Y_3Fe_5O_{12}$ based magnetic feeders in scale tank (Fig. 9). It has been observed that the magnitude of magnetic field increased by using $Y_3Fe_5O_{12}$ ferrite based magnetic feeders with aluminium EM transmitter. It can be seen that aluminuim transmitter with $Y_3Fe_5O_{12}$ ferrite based magnetic feeders gave (841nT) than without magnetic feeders (300nT) as shown in Table 3. It was found that magnitude of B field increased upto 180% with $Y_3Fe_5O_{12}$magnetic feeders.

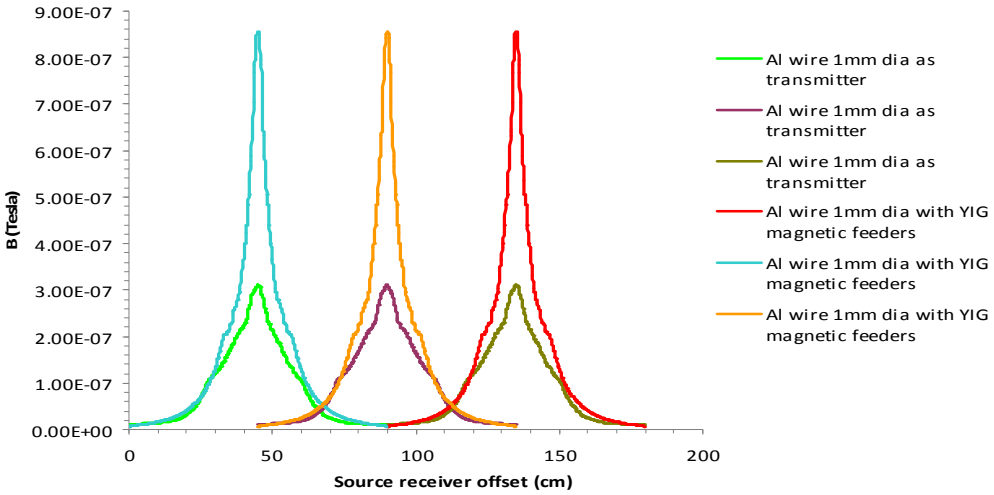

Fig. 9, Comparison of magnitude of B field vs source receiver offset of Al transmitter and new Al transmitter with $Y_3Fe_5O_{12}$ (YIG) magnetic feeders at 1150°C in lab scaled tank.

Table. 3: Comparison of MVO results of Al transmitter with and with out $Y_3Fe_5O_{12}$ magnetic feeders

	Al transmitter with out magnetic feeders	**Al transmitter with $Y_3Fe_5O_{12}$ magnetic feeders**
B-Field	3.0×10-7	8.41×10-7

Conclusion

Nanoparticles of $Y_3Fe_5O_{12}$ were successfully synthesized by using self combustion technique. XRD result reveals that crystallization begins to start at sintering temperature of 950°C where as single phase yttrium iron garnet structure with major peak [420] has been developed at low sintering temperature of 1150°C. Raman results also shows confirmation of yttrium iron garnet phase at sintering temperature of 1150°C. FESEM results showed that yttrium iron garnet has average grain size between 60 to 110nm with better morphology at sintering temperature of 1150°C. It was observed that high Initial permeability (58.054), Q factor (59.842) with low loss factor (0.0003) shows yttrium iron garnet good nanomaterials for seabed logging application. It was investigated that new Al transmitter with $Y_3Fe_5O_{12}$ magnetic feeders has ability to increase 180% magnitude of magnetic field.

References

[1] L. O. Loseth, H. M. Pedersen, S. Pettersen, T. S. Ellingsrud, T. Eidesmo, A scaled experiment for the verification of the Seabed Logging method, J. Appl. Geophys. 64, 47–55 (2008).

[2] M. N. Akhtar, N. Yahya, K. Koziol, N. Nasir, Synthesis and characterizations of $Ni_{0.8}Zn_{0.2}Fe_2O_4$-MWCNTs composites for their application in seabed logging, Ceram. Int. 37 (2011) 3237-3245.

[3] M. N. Akhtar, N. Yahya, P. B. Hussain, Structural and magnetic characterizations of nano structured $Ni_{0.8}Zn_{0.2}Fe_2O_4$ prepared by self combustion method, Int. J. Basic & App. Sci. (IJBAS). 9 (2009) 151-154.

[4] S. Ellingsrud, T. Eidesmo, S. Johansen, Remote sensing of hydrocarbon layers by seabed logging (SBL) results from a cruise offshore Angola, The leading Edge. 21 (2002) 972-982.

[5] F. N. Kong, H. Westerdah, F. Antonsen, Excitation of a long wire antenna-Antennas from 200 MHz to 1 Hz, Tenth International conference on Ground Penetrating Radar; 21 -24 June, Delft, The Netherlands (2004).

[6] M. A. Gilleo, Ferromagnetic Materials: *A handbook of the preparation of magnetically ordered substances*, E.P. Wohlfarth, North-Holland, Amsterdam (1980).

[7] M. V. Kunzentsov, Q. A. Pankhurst, I. P. Parkin, L. Affeck, Y. K. Morozov, Self-propagating high temperature synthesis of yttrium iron chromium garnets $Y_3Fe_{5-x}Cr_xO_{12}$ ($0 \leq x \leq 0.6$), J. Mater. Chem. 10 (2000) 755.

[8] Z. A. Motlagh, M. Mozaffari, and J. Amighan, Preparation of nano-sized Al-substituted yttrium iron garnets by the mechanochemical method and investigation of their magnetic properties, J. Magn. Mag. Mater, 321 (2009) 1980-1984.

[9] A. Habishi, R. Yahya, N. Shafie, M. S. E. Ismail, I. Waje, S. B. Saad, Preparation and characterization of aluminum substitute yttrium iron garnet nanoparticles by sol-gel technique, Int. Advanced Tech. Cong. (ATCI) (2005) 577-583.

[10] P. Vaqueiro, M. P. C. Lopez, M. A. L. Quintela, Annealing dependence of magnetic properties in nanostructured particles of yttrium iron garnet prepared by citrate gel, process J. Sol. Sta. Chem. 126 (1996) 161-168.

[11] N. Yahya, R. A. H. Masoud, M. Zaid, Synthesis of $Al_3Fe_5O_{12}$ cubic structure by extremely low sintering temperature of sol gel technique, Am. J. Eng. App. Sci. 2 (2009)76-79.

[12] J. L. Rehspringer, J. Burik, D. Niznansky, A. klarkora, Characterisation of bismuth-doped yttrium iron garnet layers prepared by sol–gel process, J. Magn. Magn .Mater. 211 (2000) 291-295.

[13] M. L. Wang, Z. W. Shih, C. H. Lin, Reaction mechanism of producing barium hexaferrites from γ-Fe_2O_3 and $Ba(OH)_2$ by hydrothermal method, J. Cryst. Growth. 114 (1991) 435.

[14] J. Ding, H. Yang, W. F. Miao, P. G. Mccormick, R. Street, High coercivity Ba hexaferrite prepared by mechanical alloying, J. Alloys. Compd. 221 (1995) 70.

[15] H. Tang, Y. W. Du, Z. Q. Qiu, J. C. Walker, Mossbauer investigation of zinc ferrite particles, J. Appl. Phys.63 (1988) 4105.

[16] E. Lucchini, S. Meriani, G. Sloker, Sintering of glass bonded ceramic barium hexaferrite magnetic powders, J. Mater. Sci. 18 (1983) 331.

[17] S. Deka, P. A. Joy, Characterization of nanosized NiZn ferrite powders synthesized by an autocombustion method, Mat.Che.Phys. 100 (2006) 98-101.

[18] F. X. Liu, T. Z. Li, H. G. Zhang, Structure and magnetic properties of $SnFe_2O_4$ nanoparticles, Phys. Lett. A. 323 (2004) 305.

[19] S. H. Vajargah, H. R. Madaah, Hosseini, Z. A. Nemati, Preparation and characterization of yttrium iron garnet (YIG) nanocrystalline powders by auto-combustion of nitrate-citrate gel, J. Alloys. Compd. 430 (2007) 339-343.

[20] M. N. Akhtar, N. Yahya, H. Daud, A. Shafie, H. M. Zaid, M. Kashif, N. Nasir, Development of EM wave guide amplifier potentially used for sea bed logging (SBL), J. Appl. Sci. 11 (2011) 1361–1365.

[21] N. Yahya, M. N. Akhtar, N. Nasir, A. Shafie, M. S. Jabeli, K. Koziol, CNT Fibres/Aluminium-$NiZnFe_2O_4$ based EM transmitter for improved magnitude vs. offset (MVO) in a scaled marine environment, J. Nanosci. Nanotechnol. 12 (2012) 8100-8109.

[22] D. S. Parasins, *Principles of Applied Geophysics*, Fifth ed, Chapman & Hall, (1997).

[23] M. Rajendran, S. Deka, P. A. Joy, A. K. Bhattacharya, Size-dependent magnetic properties of nanocrystalline yttrium iron garnet powders, J. Magn. Magn. Mater. 301 (2006) 212-219.

[24] M. P. Horvath, Microwave applications of soft ferrite, J. Magn. Magn. Mater. 215 (2006) 171- 183.

[25] S. Verma, S. D. Pradhan, R. Pasricha, S. R. Sainkar, P. A. Joy, A Novel Low Temperature Synthesis of Nanosized NiZn Ferrite, J. Am. Cer. Soc. 88 (2005) 2597-2599.

[26] S. H. Vajargah, H. R. M. Hosseini, Z. A. Nemati, Preparation and characterization of nanocrystalline misch-metal-substituted yttrium iron garnet powder by the sol–gel combustion process, Int. J. Appl. Ceram. Technol. 5 (2008) 464-468.

[27] J. P. Ganne, R. Lebourgeois, M. Pate, D. Dubreuil, L. Pinier, H. Pascard, The electromagnetic properties of Cu-substituted garnets with low sintering temperature, J. Eur. Cer. Soc. 27 (2007) 2771-2777.

[28] Z. Abbas, R.M. Al-habashi, K. Khalid, M. Maarof, Garnet Ferrite ($Y_3Fe_5O_{12}$) Nanoparticles Prepared via Modified Conventional Mixing Oxides (MCMO) Method, Eur. J. Sci. Res. 36 (2009) 154-160.

[29] E. C. Snelling, *Soft ferrites*. Second ed, Butterworths, London, 1998.

[30] J. J. Shrotri, S. D. Kulkarni, C. E. Deshpande, A. Mitra, S. R. Sainkar, P. S. A. Kumar, S. K. Date, Effect of Cu substitution on the magnetic and electrical properties of Ni–Zn ferrite synthesised by soft chemical method, Mater. Chem. Phys. 59 (1999)1-5.

[31] R. V. Mangalaraja, S. Ananthakumar, P. Manohar, F. D. Gnanam, Electrical and Dielectric Behaviour of $Ni_{0.8}Zn_{0.2}Fe_2O_4$ Prepared Through Flash Combustion Technique, Mat. Sci. Eng. A. 55 (2003) 320-324.